ELSEVIER

Ceramics International 30 (2004) 1647–1653

CERAMICS INTERNATIONAL

www.elsevier.com/locate/ceramint

# Microstructure and current–voltage characteristics of $ZnO–V_2O_5–MnO_2$ varistor system

H.H. Hng*, P.L. Chan

*School of Materials Engineering, Nanyang Technological University, Nanyang Avenue, Singapore 639798, Singapore*

Received 19 November 2003; received in revised form 18 December 2003; accepted 22 December 2003

Available online 6 May 2004

**Abstract**

The effects of sintering temperature and time on the microstructure and the electrical properties have been studied in a ZnO–0.5 mol%$V_2O_5$–2 mol%$MnO_2$ system. The microstructure of the samples consists mainly of ZnO grains with $Zn_3(VO_4)_2$ as the minority secondary phase. This minor secondary phase disappears for samples sintered at 1200 °C and above. An increase in sintering temperature also brings about a deleterious effect on the non-linear coefficient and the breakdown electric field. An optimum sintering time of 4 h at 900 °C gives the best electrical properties, with the non-linear coefficient $\alpha$ attaining a highest value of 31.8. Grain growth process is also investigated in terms of the phenomenological kinetic grain growth expression: $G^n = K_o t \exp(-Q/RT)$. The kinetic grain growth exponent $n$ is observed to be 4, while the apparent activation energy $Q$ is 193 ± 19 kJ/mol.


*Keywords:* A. Sintering; B. Microstructure-final; C. Electrical properties; D. ZnO; E. Varistors

## 1. Introduction

Non-ohmic behaviour of zinc oxide ceramics is achieved by adding small amounts of other metal oxides, which can be classified into three general categories, as suggested by Gupta [1]. One of these is termed "varistor formers", which consists of oxides without which varistor behaviour cannot be obtained. It was believed that effective varistor forming ingredients are heavy elements with large ionic radii, such as Bi [2,3] and Pr [4,5]. However, recent studies have now shown that $V_2O_5$, which is a light-metal oxide, is a promising varistor former [6–15]. The ZnO–$V_2O_5$ ceramic system can be sintered at a relatively low temperature of about 900 °C, which makes it possible for a varistor to be cofired with a silver inner-electrode whose melting point is about 960 °C. This is important for applications in multilayer components.

In our previous work [15], we reported the effects of $MnO_2$ content on the ZnO–0.5 mol%$V_2O_5$ binary system sintered at 900 °C for 4 h in air. It was found that 2 mol%$MnO_2$ gives the optimum electrical properties. In this work, the microstructure and grain growth in ZnO–0.5 mol%$V_2O_5$–2 mol%$MnO_2$ ceramics were investigated as a function of sintering temperature and time. The results of a study of the current density–electric field ($J$–$E$) behaviour in these ceramics are also reported.

## 2. Experimental procedures

High purity oxide powder starting materials were used for the preparation of the ZnO varistor samples. $MnO_2$ (2 mol%) was mixed with a mixture of ZnO–0.5 mol%$V_2O_5$ powder by ball milling with alumina balls and deionised water for 24 h. The mixtures were then dried and pressed into pellets. The pellets were then sintered in an atmosphere of ambient air for different times (1, 2, 4, 6 and 8 h) at 900 °C, and at different temperatures (900, 1000, 1100, 1200, 1300 °C) for 4 h with heating and cooling rates of 5 °C/min.

For electrical measurements, the as-sintered specimens were lapped on both surfaces to ensure flat and parallel surfaces. They were coated with conductive silver paint on both surfaces, then heat cured to provide ohmic contacts. The $I$–$V$ characteristics were determined at room temperature using a variable dc power supply (Kikusui Withstanding Voltage Tester, TOS 5051). X-ray analysis of the sintered

* Corresponding author. Tel.: +65-67904140; fax: +65-67909081.
*E-mail address:* ashhhng@ntu.edu.sg (H.H. Hng).

0272-8842/$30.00 
doi:10.1016/j.ceramint.2003.12.162

samples was carried out using Cu Kα radiation on a powder diffractometer (Shimadzu XRD-6000). Microstructures of polished and etched specimens were examined by SEM (JEOL JSM 5310) equipped with energy dispersive X-ray analysis (EDX). Average ZnO grain size was measured by the intercept method with a multiplying factor of 1.56 [16].

## 3. Results and discussion

### 3.1. X-ray powder diffraction (XRPD)

XRPD traces for samples sintered at various temperatures are shown in Fig. 1. For samples sintered at temperatures ≤1100 °C, other than the major ZnO phase, $Zn_3(VO_4)_2$ was the only secondary phase detected. However, this minor secondary phase disappeared when the sintering temperature was increased to 1200 °C or higher. The appearance of the $Zn_3(VO_4)_2$ phase is consistent with earlier reports of $V_2O_5$-doped ZnO ceramics sintered at 900 °C [7,12–15].

It is also noted that the type of $Zn_3(VO_4)_2$ polymorphs formed is dependent on the sintering temperature. γ-$Zn_3(VO_4)_2$ phase was formed in samples sintered at 900 °C, while α-$Zn_3(VO_4)_2$ phase was formed in samples sintered at 1000 and 1100 °C. In our earlier studies, it was also found that the type of $Zn_3(VO_4)_2$ polymorphs formed in the $V_2O_5$-doped ZnO varistors is dependent on the $V_2O_5$ content, as well as on the type of additives oxides introduced into the system [12,13]. It was reported that the γ-$Zn_3(VO_4)_2$ and α-$Zn_3(VO_4)_2$ phases were detected in ZnO–$V_2O_5$–$MnO_2$ and ZnO–$V_2O_5$–$Co_3O_4$, respectively, while in the ZnO–$V_2O_5$–$MnO_2$ system, when the amount of $V_2O_5$ is ≤0.5 mol%, only γ-$Zn_3(VO_4)_2$ was detected in the samples. For samples containing >0.5 mol%$V_2O_5$, both the β- and γ-$Zn_3(VO_4)_2$ phase were detected. It was also suggested that the existence of this minority secondary phase have an effect on the electrical properties. This will be further discussed in Section 3.3.

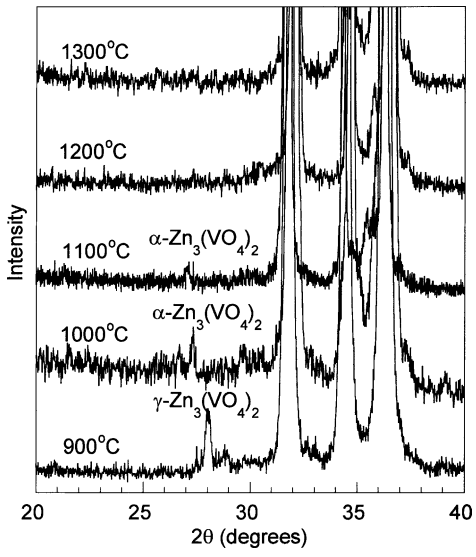


Fig. 1. XRPD traces (Cu Kα) for ZnO–$V_2O_5$–$MnO_2$ samples sintered at different temperatures, indicating the disappearance of the γ-$Zn_3(VO_4)_2$ phase at sintering temperatures 1200 °C or higher.

XRD analysis was also performed on the samples sintered at 900 °C for various lengths of time. It was found that sintering time has no significant effect on the type of $Zn_3(VO_4)_2$ polymorphs formed. Only the γ-$Zn_3(VO_4)_2$ phase was detected as the minor secondary phases in this set of samples.

### 3.2. Microstructure and grain growth

The typical microstructure of the ZnO–0.5 mol%$V_2O_5$–2 mol%$MnO_2$ samples sintered at various temperatures and times are shown in Figs. 2 and 3. Consistent with previous studies [13,15], the incorporation of $MnO_2$ did not seem to affect the general microstructure of $V_2O_5$-doped ZnO ceramics, other than the dissolution of Mn in the ZnO grains, which is believed to have considerable importance for the electrical properties of varistors by acting as dopants [13,15]. The microstructures of the sintered showed the following features: (1) large grains dispersed in a matrix composed of small grains and (2) the large grains having oblong shape. The microstructural observations are consistent with the reported liquid-phase sintering mechanism for ZnO varistors containing $V_2O_5$, which gives rise to exaggerated ZnO grain growth [6–15]. ZnO has a eutectic reaction with $Zn_3(VO_4)_2$ at ~890 °C [17], and for sintering at ≥900 °C, it has been suggested that the liquid phase $Zn_3(VO_4)_2$ enhances densification by solution and reprecipitation of ZnO [7].

In general, the ZnO grain size is observed to increase with increasing temperature and time. In addition, the average grain sizes are much larger than those of pure zinc oxide (3.7 μm) that was sintered at 900 °C for 4 h [8]. However, it is observed that for samples sintered at temperatures ≥1000 °C or for longer sintering times, a more uniform microstructure is observed. The ZnO grain growth behaviour of the ZnO–$V_2O_5$–$MnO_2$ system is studied using the phenomenological kinetic grain growth expression [18]

$$G^n = K_o t \exp\left(-\frac{Q}{RT}\right) \quad (1)$$

where $G$ is the average grain size at time $t$; $n$, kinetic grain growth exponent; $K_o$, pre-exponential constant of the material; $Q$, apparent activation energy; $R$, universal gas constant and $T$ is the absolute temperature.

The phenomenological kinetic grain growth equation can be readily plotted in the form

$$\ln G = \frac{1}{n}\ln t + \frac{1}{n}\left(\ln K_o - \frac{Q}{RT}\right) \quad (2)$$

From the slope of the $\ln G$ versus $\ln t$ line, which is $1/n$, the grain growth kinetic exponent is determined. Fig. 4 illustrates the isothermal grain growth results for the ZnO–0.5 mol%$V_2O_5$–2 mol%$MnO_2$ samples sintered at 900 °C in the form of Eq. (2). The slope is found to be

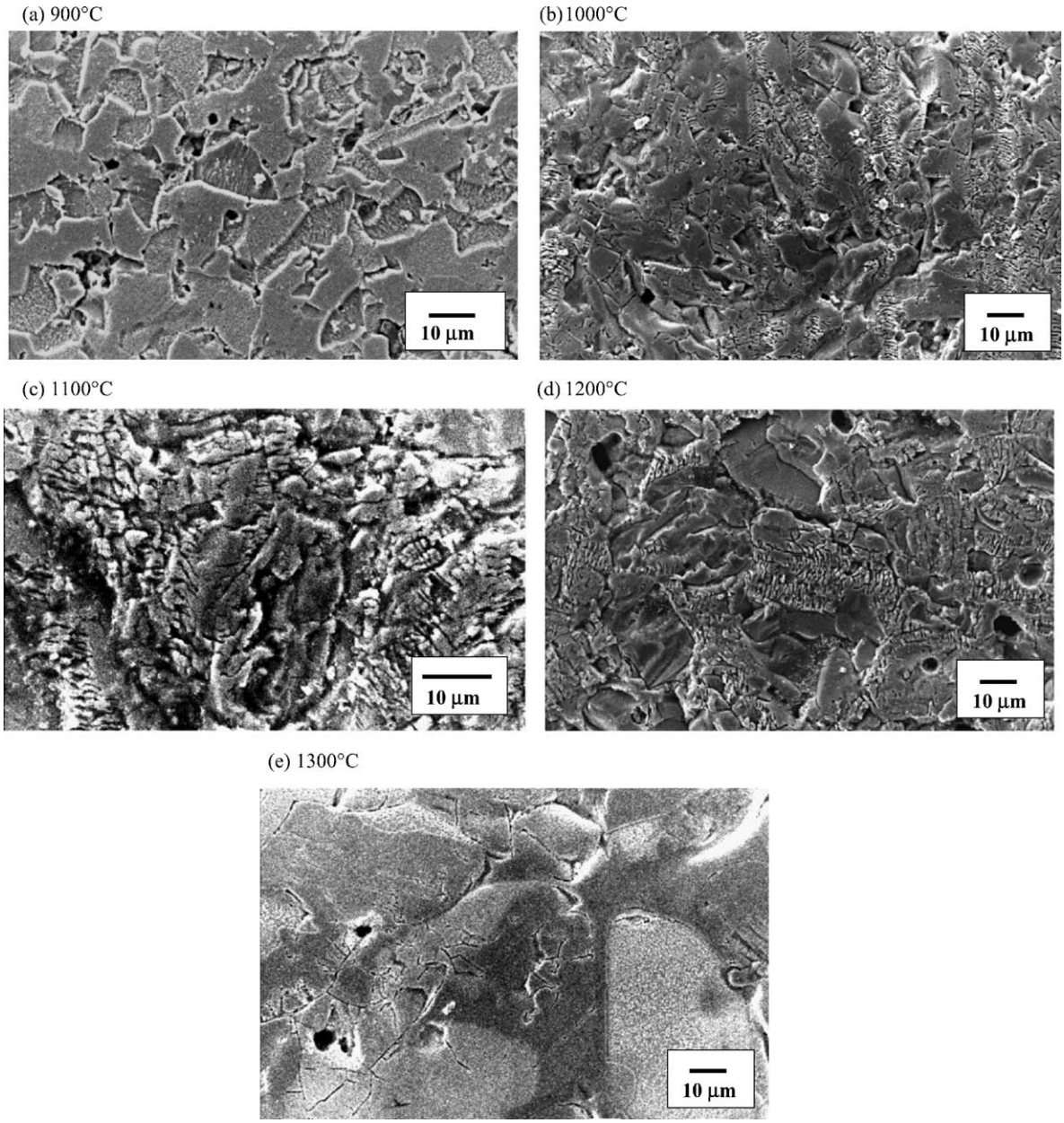


Fig. 2. SEM micrographs of ZnO–0.5 mol%$V_2O_5$–2 mol%$MnO_2$ samples sintered for 4 h at (a) 900 °C, (b) 1000 °C, (c) 1100 °C, (d) 1200 °C and (e) 1300 °C.

0.25, yielding a grain growth exponent $n$ of 4. This value of $n$ is slightly higher compared to the value of 3 for pure ZnO [18]. However, Tsai and Wu [8] obtained $1/n$ values ranging from 0.63 to 0.83 (equivalent to $n$ values of 1.20 to 1.59) for their ZnO–$V_2O_5$ binary systems with $V_2O_5$ content varying from 0.5 to 2.0 mol%. Similar $n$ values ranging from 1.52 to 1.79 were also obtained for ZnO–$V_2O_5$ binary systems with $V_2O_5$ content varying from 0.5 to 2.0 mol% in an earlier study [19]. It was suggested that the small $n$ values indicate a fast growing behaviour, and that the changes in the ZnO grain growth rate after doping with $V_2O_5$ is due to the presence of the liquid phase $Zn_3(VO_4)_2$, which enhances densification by solution and reprecipitation of ZnO during sintering. In the current study with 2 mol%$MnO_2$ added to a ZnO–0.5 mol%$V_2O_5$ system, the $n$ value of 4 is higher than that of pure ZnO and binary ZnO–$V_2O_5$ systems. Large grain growth exponents are indicative of slowly coarsening microstructures, for the rate of grain growth ($dG/dt$ or $d(\ln G)/dt$), decreases with increasing $n$ value, as can be readily seen by differentiating Eq. (2). The decrease in the rate of ZnO grain growth with the addition of $MnO_2$, may be due to the dissolution of Mn in the ZnO grains. The presence of Mn in ZnO may affect the solution–precipitation liquid phase sintering, and decrease the rate of ZnO grain growth during sintering.

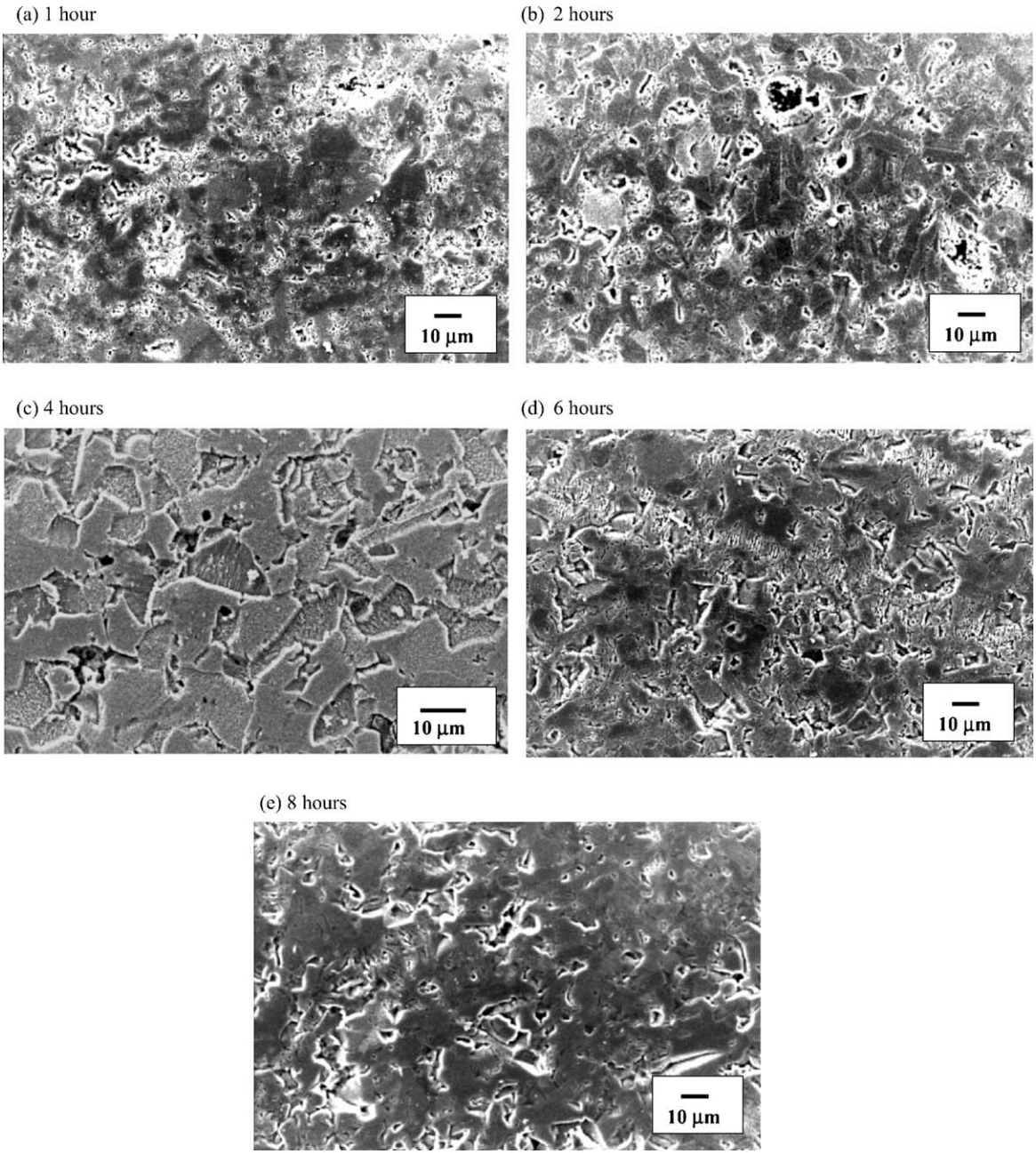


Fig. 3. SEM micrographs of ZnO–0.5 mol%$V_2O_5$–2 mol%$MnO_2$ samples sintered at 900 °C for (a) 1 h, (b) 2 h, (c) 4 h, (d) 6 h and (d) 8 h.

The grain growth in the ZnO–$V_2O_5$–$MnO_2$ system is also shown from its apparent activation energy obtained from the Arrhenius plot of $\ln(G^4/t)$ versus the reciprocal of the absolute temperature $1/T$ (Fig. 5). There exists a reasonably good linear relationship between $\ln(G^4/t)$ and $1/T$ from 900 to 1300 °C, implying that the mechanism for grain growth is the same in this temperature range. The apparent activation energy for the ZnO–$V_2O_5$–$MnO_2$ system was calculated from the slope to be $193 \pm 19$ kJ/mol. This apparent activation energy is lower than that of pure ZnO, which has a value of 224 kJ/mol [18], but higher than that of binary ZnO–$V_2O_5$ systems ($V_2O_5$ content: $\leq$2 mol%), which has an average value of about 88 kJ/mol [19].

From the same plot, the value of the pre-exponential constant, $K_o$, was also determined and found to be $1.08 \times 10^{12}$ μm$^4$/h. The pre-exponential constant is reported to contain the concentration of the solid in the liquid, the atomic volume of the solid, the solid–liquid surface energy, and either the interface reaction rate constant or the diffusivity of the solid through liquid, depending on the rate-controlling process [20]. Unfortunately, this pre-exponential factor cannot be directly compared to that of ZnO, which has a value of $2.95 \times 10^{11}$ μm$^3$/h [18], due to the different units.

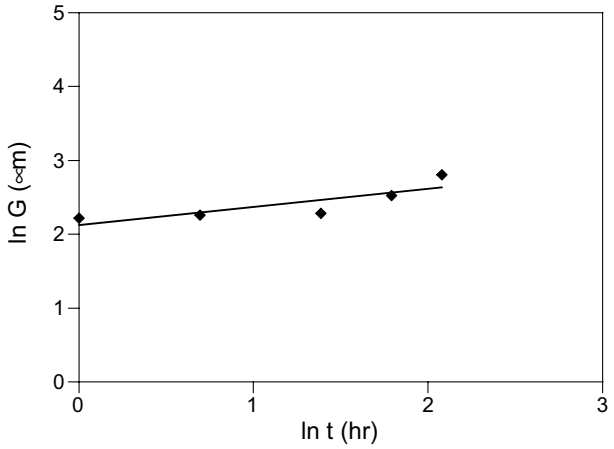


Fig. 4. ZnO grain growth in ZnO–0.5 mol%$V_2O_5$–2 mol%$MnO_2$ ceramics sintered at 900 °C for various sintering times.

### 3.3. Current–voltage characteristics

The effects of sintering temperature and time on the electrical properties of the ZnO–0.5 mol%$V_2O_5$–2 mol%$MnO_2$ materials were characterised by their electric field–current density (*E–J*) properties. Typical *E–J* curves are shown in Fig. 6. The corresponding parameters obtained from these curves are summarised in Table 1, where the point at which non-linearity begins is given by the onset electric field $E_{1\,mA/cm^2}$ and leakage current density $J_{leak}$.

The breakdown electric field, $E_{1\,mA/cm^2}$, and the non-linear coefficient, $\alpha$ decreased significantly as the sintering temperature increases from 900 to 1100 °C. The leakage current, $J_{leak}$, however, remained relatively constant. For sintering temperatures ≥1200 °C, the varistor effect was lost. Similar decrease in the breakdown field and the non-linear coefficient with increasing sintering temperature were also observed by other workers in their $V_2O_5$-doped ZnO ceramic system [7,9].

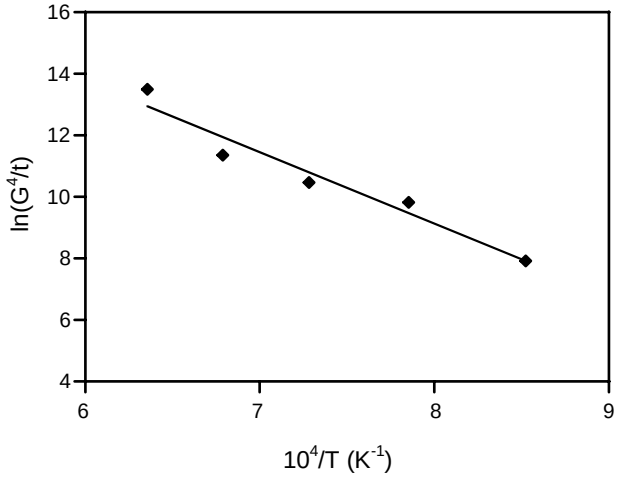


Fig. 5. Arrhenius plot for ZnO grain growth in ZnO–0.5 mol%$V_2O_5$–2 mol%$MnO_2$ ceramics.

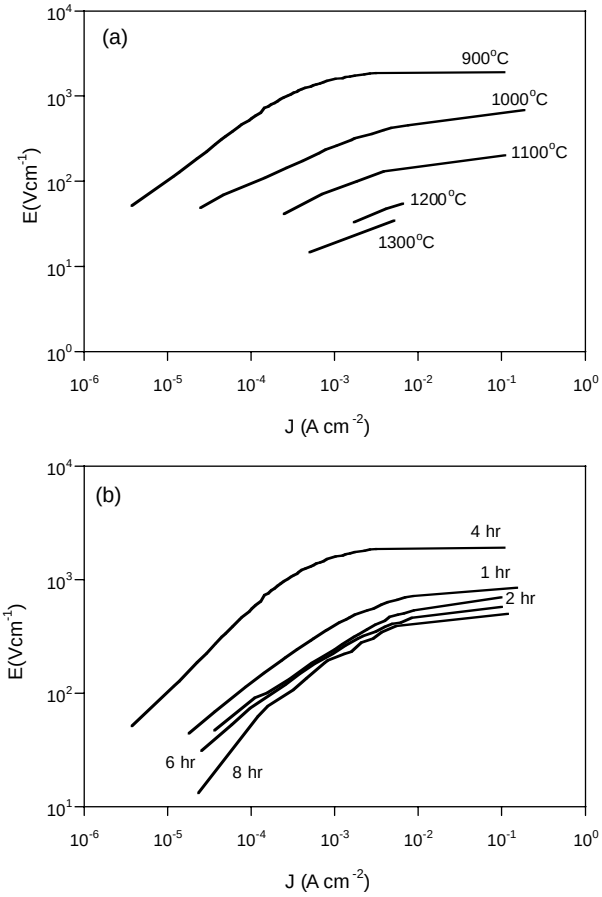


Fig. 6. The electric field–current density (*E–J*) curves for the various ZnO–0.5 mol%$V_2O_5$–2 mol%$MnO_2$ ceramics sintered at various (a) temperatures and (b) times.

At present, as we have stated elsewhere [13], there is no unique model that can predict quantitatively ZnO varistor *I–V* behaviour from a knowledge of the microstructure. Only a qualitative explanation is possible. Levinson and Philipp [21] have pointed out that, in practice, there are a variety of inter-grain conduction paths that operate in parallel in varistors. These can be through the grain boundary region or through the bulk intergranular material, and are sensitive to the presence of chemical additives. For $V_2O_5$-doped ZnO varistors, conduction can occur through the V-rich intergranular layers containing different chemical additives, as well as through the minor secondary phases such as $Zn_3(VO_4)_2$ residing at grain boundaries and triple junctions [13]. The rapid deterioration of the varistor effect with sintering temperature may be related to the type of $Zn_3(VO_4)_2$ polymorph present in the sintered samples. In a previous study, the experimental results suggested that the secondary phase $Zn_3(VO_4)_2$ plays a role in the electrical performance of ZnO–$V_2O_5$ varistor [13]. It was found that it is desirable to have γ-$Zn_3(VO_4)_2$ rather than the α- or β-$Zn_3(VO_4)_2$ as a secondary phase, due to its lower conductivity. The α-$Zn_3(VO_4)_2$ phase was detected in our samples that were sintered at temperatures >900 °C, while the γ-$Zn_3(VO_4)_2$ phase existed in the sample

Table 1
Summary of varistor parameters for ZnO–$V_2O_5$–$MnO_2$ ceramics sintered at various temperatures and times

| Sintering temperature (°C) | Sintering time (h) | Average ZnO grain size (μm) | $E_{1\,mA/cm^2}$ (V/cm)[a] | $J_{leak}$ (A/cm$^2$)[b] | Non-linear coefficient ($\alpha$)[c] |
|---|---|---|---|---|---|
| 900 | 4 | 9.8 | 2000 | $6 \times 10^{-4}$ | 31.8 |
| 1000 | 4 | 15.6 | 280 | $8 \times 10^{-4}$ | 8.1 |
| 1100 | 4 | 18.3 | 80 | $5 \times 10^{-4}$ | 7.6 |
| 1200 | 4 | 22.7 | – | – | – |
| 1300 | 4 | 38.4 | – | – | – |
| 900 | 1 | 9.2 | 400 | $7 \times 10^{-4}$ | 11.4 |
| 900 | 2 | 9.6 | 250 | $6 \times 10^{-4}$ | 9.8 |
| 900 | 6 | 12.5 | 230 | $5 \times 10^{-4}$ | 8.5 |
| 900 | 8 | 16.6 | 200 | $6 \times 10^{-4}$ | 7.8 |

[a] Electric field at 1 mA/cm$^2$.
[b] Current density at $0.8E_{1\,mA/cm^2}$.
[c] $\alpha = \log(J_2/J_1)/\log(E_2/E_1)$ where $J_1 = 10\,mA/cm^2$ and $J_2 = 100\,mA/cm^2$.

sintered at 900 °C. Thus, this explains why the samples sintered at 900 °C exhibited better varistor behaviour. Moreover, the absence of the varistor effect for samples sintered at temperatures above 1200 °C can be attributed to the absence of the $Zn_3(VO_4)_2$ phase in these samples. Our results further confirms the important role played by the $Zn_3(VO_4)_2$ secondary phase in the electrical performance of $V_2O_5$-doped ZnO ceramics.

Sintering time also greatly influenced the breakdown electric field, $E_{1\,mA/cm^2}$ and non-linear coefficient $\alpha$, while not significantly affecting the leakage current density, $J_{leak}$, of the ZnO–0.5 mol%$V_2O_5$–2 mol%$MnO_2$ ceramics. An exceptionally high $E_{1\,mA/cm^2}$ and $\alpha$ values were obtained for samples sintered for 4 h. Tsai and Wu [8] also found that a largest $\alpha$ value occurred at 4 h of sintering for their ZnO–$V_2O_5$ binary materials. They suggested that such observation might be correlated with the abnormal granular microstructure, in that a skeleton of lower resistance paths for the exaggerated grains was present after this time of sintering.

## 4. Conclusions

Sintering temperature and time have an adverse effect on the microstructure and the electrical properties in the ZnO–0.5 mol%$V_2O_5$–2 mol%$MnO_2$ system. For samples sintered at temperature $\leq$1100 °C, the microstructure consists mainly of ZnO grains with $Zn_3(VO_4)_2$ as the minority secondary phase. The $Zn_3(VO_4)_2$ phase disappeared when the sintering was increased to 1200 °C and above. An increase in sintering temperature also brought about a deleterious effect on the non-linear coefficient and the breakdown electric field. Such behaviour can be correlated to the $Zn_3(VO_4)_2$ secondary phase, and the type of $Zn_3(VO_4)_2$ polymorph that existed in the samples. An optimum sintering time of 4 h at 900 °C gave the best electrical properties, with the non-linear coefficient $\alpha$ attaining a highest value of 31.8.

Grain growth process in the liquid-phase-sintered ZnO–0.5 mol%$V_2O_5$–2 mol%$MnO_2$ ceramics was also investigated. The average grain size increased proportionally to the one-fourth power of the time, a kinetic grain growth exponent of 4, and with an apparent activation energy for grain growth of $193 \pm 19$ kJ/mol.

## References

[1] T.K. Gupta, Microstructural engineering through donor and acceptor doping in the grain and grain boundary of a polycrystalline semiconducting ceramic, J. Mater. Res. 7 (1992) 3280–3295.
[2] M. Matsuoka, Non-ohmic properties of zinc oxide ceramics, Jpn. J. Appl. Phys. 10 (1971) 736–746.
[3] J. Wong, Sintering and varistor characteristics of ZnO–$Bi_2O_3$ ceramics, J. Appl. Phys. 51 (1980) 4453–4459.
[4] K. Mukae, K. Tsuda, I. Nagasawa, Non-ohmic properties of ZnO–rare earth metal oxide–$Co_3O_4$ ceramics, Jpn. J. Appl. Phys. 16 (1977) 1361–1368.
[5] A.B. Alles, V.L. Burdick, The effect of liquid-phase sintering on the properties of $Pr_6O_{11}$-based ZnO varistors, J. Appl. Phys. 70 (1991) 6883–6890.
[6] J.K. Tsai, T.B. Wu, Non-ohmic characteristics of ZnO–$V_2O_5$ ceramics, J. Appl. Phys. 76 (1994) 4817–4822.
[7] J.K. Tsai, T.B. Wu, Microstructure and non-ohmic properties of ZnO–$V_2O_5$ ceramics, Jpn. J. Appl. Phys. Part 1 34 (1995) 6452–6457.
[8] J.K. Tsai, T.B. Wu, Microstructure and non-ohmic properties of binary ZnO–$V_2O_5$ ceramics sintered at 900 °C, Mater. Lett. 26 (1996) 199–203.
[9] C.S. Chen, C.T. Kuo, T.B. Wu, I.N. Lin, Microstructure and electrical properties of $V_2O_5$-based multicomponent ZnO varistors prepared by microwave sintering process, Jpn. J. Appl. Phys. Part 1 36 (1997) 1169–1175.
[10] C.T. Kuo, C.S. Chen, I.N. Lin, Microstructure and non-linear properties of microwave-sintered ZnO–$V_2O_5$ varistors: I. Effect of $V_2O_5$ doping, J. Am. Ceram. Soc. 81 (1998) 2942–2948.
[11] C.T. Kuo, C.S. Chen, I.N. Lin, Microstructure and non-linear properties of microwave-sintered ZnO–$V_2O_5$ varistors: II. Effect of $Mn_3O_4$ doping, J. Am. Ceram. Soc. 81 (1998) 2949–2956.
[12] H.H. Hng, K.M. Knowles, Characterisation of $Zn_3(VO_4)_2$ phases in $V_2O_5$-doped ZnO varistors, J. Eur. Ceram. Soc. 19 (1999) 721–726.

[13] H.H. Hng, K.M. Knowles, Microstructure and current–voltage characteristics of multi-component vanadium-doped zinc oxide varistors, J. Am. Ceram. Soc. 83 (2000) 2455–2462.
[14] H.H. Hng, K.M. Knowles, P.A. Midgley, Zinc vanadates in vanadium oxide-doped zinc oxide varistors, J. Am. Ceram. Soc. 84 (2001) 435–441.
[15] H.H. Hng, P.L. Chan, Effects of $MnO_2$ doping in $V_2O_5$-doped ZnO varistor system, Mater. Chem. Phys. 75 (2002) 61–66.
[16] M.I. Mendelson, Average grain size in polycrystalline ceramics, J. Am. Ceram. Soc. 52 (1969) 443–446.
[17] J.J. Brown, F.A. Hummel, Reactions between ZnO and selected oxides of elements of Groups IV and V, Trans. Br. Ceram. Soc. 64 (1965) 419–437.
[18] T. Senda, R.C. Bradt, Grain growth in sintered ZnO and ZnO–$Bi_2O_3$ ceramics, J. Am. Ceram. Soc. 73 (1990) 106–114.
[19] H.H. Hng, K.Y. Tse, Grain growth of ZnO in binary ZnO–$V_2O_5$ ceramics, J. Mater. Sci. 38 (2003) 2367–2372.
[20] D. Dey, R.C. Bradt, Grain growth of ZnO during $Bi_2O_3$ liquid-phase sintering, J. Am. Ceram. Soc. 75 (1992) 2529–2534.
[21] L.M. Levinson, H.R. Philipp, Zinc oxide varistor—a review, Am. Ceram. Soc. Bull. 65 (1986) 639–646.